FAR-INFRARED SOURCES AND DIFFUSE EMISSION IN M31

CONG XU
Max-Planck-Institut für Kernphysik, W6900 Heidelberg, Germany

GEORGE HELOU
IPAC 100-22, California Institute of Technology, Pasadena, CA 91125

ABSTRACT A study on the far-infrared (FIR) emission of M31 has been carried out with the HiRes maps ($\sim 1'$) derived from IRAS data. Sixty-eight FIR sources are detected in M31, which in general coincide with optical HII regions, and contribute 15%, 23%, 29%, and 23% to the fluxes in 12 μm, 25 μm, 60 μm, and 100 μm bands, respectively. The remaining diffuse emission, which dominates the FIR emission of M31, is studied using a dust heating model which utilizes the UV and optical photometry maps and the HI maps available in the literature. It is found that the global dust-to-gas ratio in M31 disk is 6.5 10^{-3}, very close to the dust-to-gas ratio in the solar neighborhood. There is a significant galactocentric gradient of the dust-to-HI-gas ratio, with an e-folding scale length of 9 kpc. The diffuse dust correlates tightly with the HI gas. The model indicates that the non-ionizing UV (913—4000Å) radiation from massive and intermediate massive stars contributes only about 30% of the heating of the diffuse dust, while the optical-NIR (4000—9000Å) radiation from the old stellar population is responsible for the most of the heating.

INTRODUCTION

Two characteristics make M31 unique for a far-infrared (FIR) study. The first is its proximity: Being the nearest spiral galaxy outside the Milky Way, it offers the best linear resolution for observations of spirals with a given angular resolution. This is a significant advantage given the relatively poor angular resolutions of the current generation of FIR instruments. Second, it is known to have very low current star-formation rate, perhaps an order of magnitude lower than that of the Milky Way (Walterbos 1988). Not many such quiescent spirals can be studied in the FIR, and none beside M31 with such high spatial resolution.

The FIR emission of M31 has been studied by Habing et al. (1984), Soifer et al. (1985), and very extensively by Walterbos and Schwering (1987) using IRAS maps. We report preliminary results from a new study using the HiRes maps. Our emphasis is to study the properties of FIR sources and the diffuse emission separately. This was not possible in the previous studies because of the relatively coarse resolution of earlier maps based on IRAS observations.

S. Terebey and J. Mazzarella (eds.), *Science with High-Spatial Resolution Far Infrared Data*, 87–93, 1994, Jet Propulsion Laboratory, Pasadena, CA.

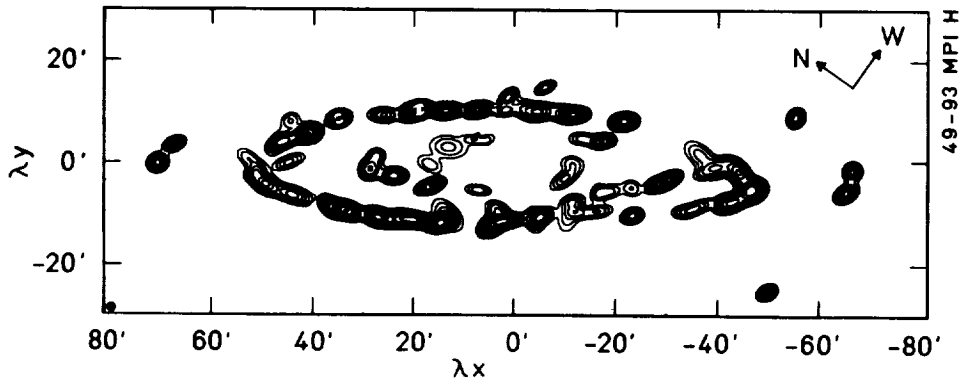

FIGURE 1 Contour map of M31 showing unresolved 60 μm sources only. The resolution has been degraded to 1.7′, indicated by the hatched circle in the lower left corner.

FIR MORPHOLOGY

The FIR morphology revealed by the HiRes maps (see Fowler and Aumann, this volume) is obviously very different from the optical morphology of M31 (Walterbos and Kennicutt 1987). Most of the FIR emission is confined in surprisingly thin arms which are hardly resolved by the HiRes beam, and in a nucleus much smaller than the optical bulge. The contrast between the arms and interarm regions is more than an order of magnitude. At similar spatial resolution, the optical emission is much smoother than the FIR emission. There is a kind of anti-correlation between the optical and FIR emission: many thin dark lanes in the optical map appear as thin bright arms in the 60 μm HiRes map.

FIR SOURCES

There are many bright sources on the 60 μm HiRes map. The brightest ones are concentrated on the famous ring at about 10 kpc (50′) galactocentric radius. Thanks to the high resolution ($\sim$ 1′), most of them are well separated from each other, so we can do a relatively clean and complete source extraction using Gaussian fitting. We found 68 60 μm sources (Figure 1), all coincident with known giant HII regions or HII region complexes (Pellet et al. 1978).

Unresolved sources account for a small fraction of the emission. They contribute 15%, 23%, 29%, and 23% to the total fluxes of M31 at 12 μm, 25 μm, 60 μm, and 100 μm, respectively. By comparison, unresolved sources in M33 contribute 50%, 92%, 68% and 56% of the total fluxes of that galaxy in the four corresponding bands (Rice et al. 1990).

In addition, the sources in M31 are not as warm as the M33 sources. Figure 2 compares the average FIR spectrum of the M31 sources to that of the M33 sources, and to the spectrum of the integrated emission of M31.

The 60 μm-to-100 μm color ratio of the M31 sources is warmer than that of the integrated emission, but significantly cooler than that of the M33 sources.

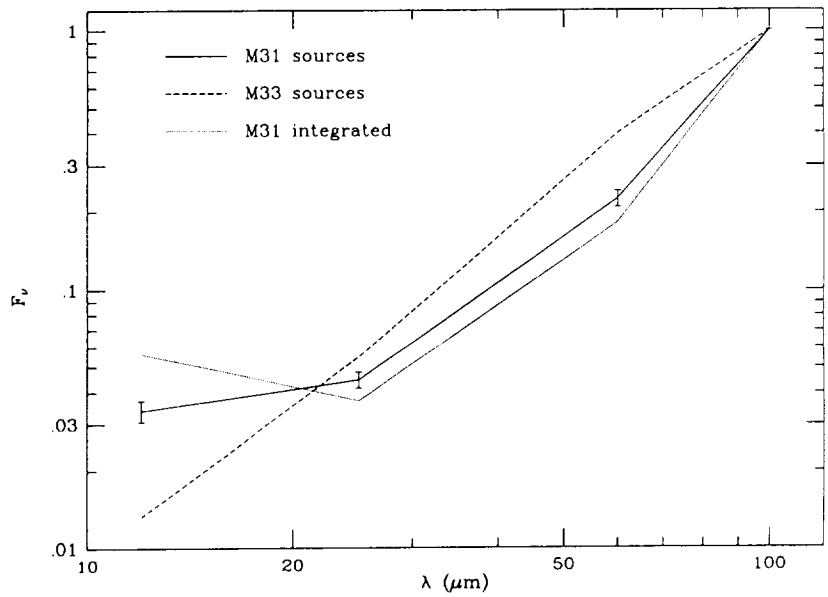

FIGURE 2 Average FIR spectrum (normalized by $F_{100\ \mu m}$) of the M31 sources (solid line) compared to that of the M33 sources (dashed line), and that of the integrated emission of M31 (dotted line).

DIFFUSE DUST

We define the diffuse component as the emission from areas in M31 where unresolved sources contribute less than 20% of the emission; the bulge area is also excluded from the following discussion. By studying this dominant component, we attempt to answer the following questions:

1. How is the interstellar dust distributed in M31? How does it correlate with HI gas?
2. How much interstellar dust does M31 have? What is the dust-to-gas ratio?
3. What is the energy budget of the diffuse interstellar dust?

We developed a dust-heating model, in which we assume that the heating of the diffuse dust is provided by the non-ionizing UV and optical interstellar radiation. We adopt an infinite-plane-parallel-slab geometry for the radiation transfer problem (van de Hulst and De Jong 1969), and assume that the dust and the UV light have the same scale height, while the scale height of the optical radiation is a factor of 2 larger. The model is applied to a complete sample of small areas (cells), each of size $2' \times 2'$, within the M31 disk. The sample selection is described in Xu and Helou (1993a). With the adopted distance (690 kpc) and inclination (13°, 90° for seen face-on), the linear size of the cells is 0.4×1.8 kpc in the plane of M31. Cells are included only if their FIR (40–120 μm) surface brightness B_{fir}, calculated from the 60 μm and 100 μm surface brightness (Helou et al. 1988), exceeds a signal-to-noise ratio of five.

The radiation transfer model predicts for each cell the ratio between the FIR surface brightness due to heating of dust by the radiation in a given band,

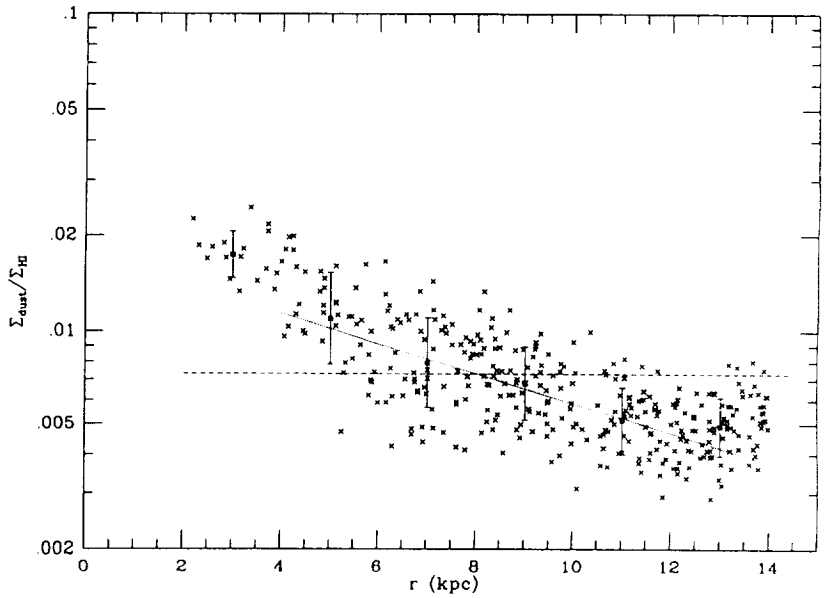

FIGURE 3 Plot of the dust-to-HI-gas ratio versus the galactocentric radius of the diffuse FIR emission in M31.

and the observed radiation surface brightness of the same band, as a function of the optical depth:

$$Q_i(\tau_{\lambda,i}) = \frac{\Delta_i B_{fir}}{B_{\lambda,i}}. \quad (1)$$

Surface brightness maps of the non-ionizing UV and the optical (UBVR) radiation have been taken from corresponding maps (Milliar 1984; Walterbos and Kennicutt 1987), and the FIR emission is assumed to be due to dust heated by the radiation in these bands:

$$B_{fir} = \sum_{i}^{5} B_i \times Q_i. \quad (2)$$

The summation of the right side of Eq.(2) is over five radiation bands: UV (912 — 3000Å, U (3000 — 4000Å), B (4000 — 5000Å), V (5000 — 6000Å), and R/NIR (6000 — 9000Å). Assuming an extinction law which is the same as the local one (Savage and Mathis 1979), the extinction at different wavelength bands depends on a single parameter, i.e., the dust column density which, consequently, can be determined using Eq.(2) (see Xu and Helou 1993b for more details).

The results of our model are shown in the following three figures. Figure 3 is the plot of the dust-to-HI-gas ratio versus the galactocentric radius.

The HI column density is taken from the HI map of Brinks (1984). The dashed line shows the dust-to-gas ratio in the solar neighborhood. It can be seen that the dust-to-HI-gas ratios of the M31 cells is not very different from the local value. The solid squares show the average value for the cells in each 2 kpc bin of galactocentric radius. The error bars represent one-σ dispersions, and amount only to about 30%. There is a clear trend that the dust-to-HI-gas

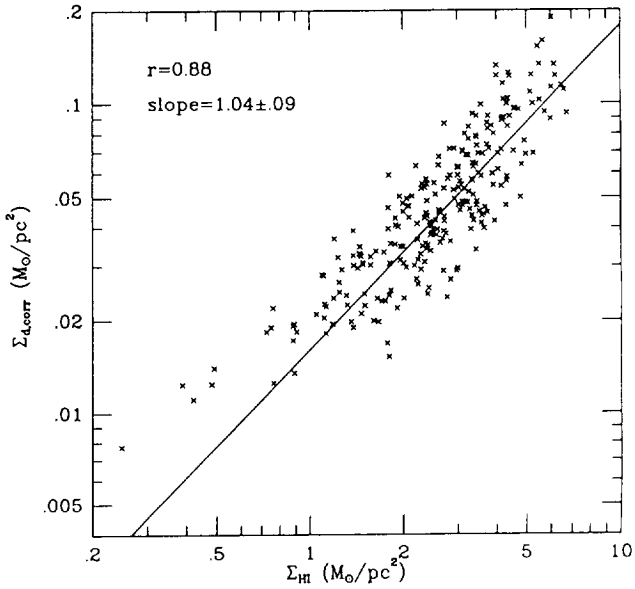

FIGURE 4 Diagram of the 'gradient-corrected' dust column density versus HI column density in the M31 disk.

ratio decreases with increasing radius, suggesting a galactocentric gradient in the dust-to-gas ratio. The set of average values can be fitted reasonably well by the dotted line, corresponding to an e-fold scale length of the gradient of 9 kpc.

Figure 4 is the diagram of the 'gradient-corrected' dust column density versus HI column density.

By 'gradient-corrected' we mean the dust column density multiplied by exp (r/9 kpc), to balance the gradient of the dust-to-gas ratio. A strong and linear correlation is found in this diagram: the correlation coefficient is 0.88 and the slope of the log-log plot is 1.04±0.09, which is shown by the solid line. Thus in M31, dust correlates tightly with the HI gas, and the local dust column density scales linearly with the column density of HI gas, while the scaling factor decreases with increasing galactocentric radius. Integrating the dust in the entire disk of M31, we find that there is 2.0 10^7 M dust within a 16 kpc radius in the M31 disk. The global dust-to-HI gas ratio is 6.6 10^{-3}, quite close to the local value of 7.3 10^{-3} (Désert et al. 1990).

In Figure 5, we compare the radial distributions of the FIR emission and of dust heating predicted by the model. The solid curve is the FIR distribution. The dashed curve is the total heating which accounts for about 80% of the FIR. The difference between the FIR emission and the heating is likely to be due to the sources. For example, the difference is most significant around the ring and in the outer region of the disk, where most of the bright sources are (Figure 1). The non-ionizing UV radiation contributes only 26% of the total heating, which is represented by the dotted-dashed curve. It is most prominent at the ring, but never dominant. Throughout the M31 disk, the optical radiation, shown as the dotted curve, dominates the heating of the diffuse dust. This indicates that the FIR emission of M31 is mainly due to heating by the optical radiation from relatively old stars, i.e., stars older than a few 10^9 years.

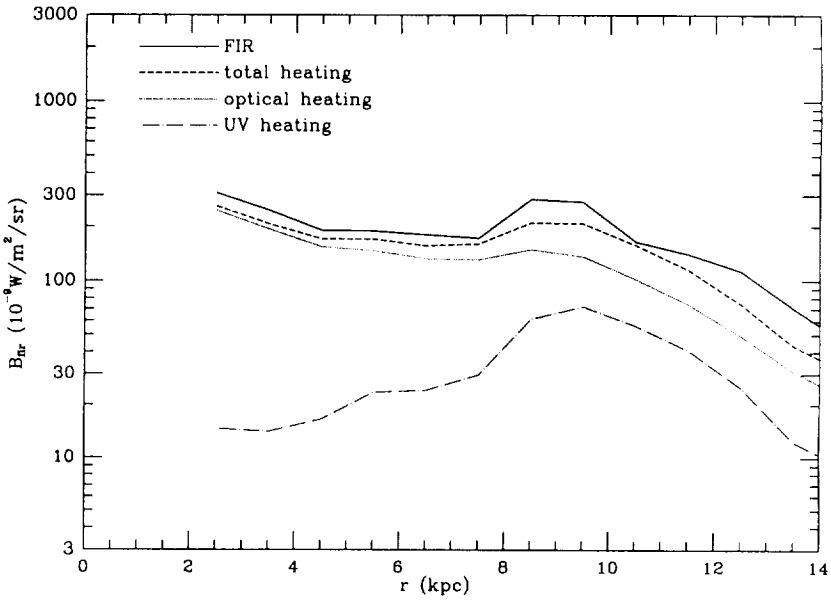

FIGURE 5 Plot of the radial distributions of the FIR emission and of dust heating predicted by the model.

ACKNOWLEDGMENTS

This work was carried out in part at the Jet Propulsion Laboratory, California Institute of Technology, under a contract with the National Aeronautics and Space Administration.

REFERENCES

Brinks, E. 1984, Ph.D. thesis, University of Leiden

Désert, F.A., Boulanger, F., and Puget, J.L. 1990, *A&A*, **273**, 215

Habing, H.J., *et al.* 1984, *ApJ*, **278**, L59

Milliard, B. 1984, These, d'Etat, University de Marseille

Pellet, *et al.* 1978, *A&AS*, **31**, 439

Rice, W., *et al.* 1990, *ApJ*, **358**, 418

Savage, B.D. and Mathis, J.S. 1979, *ARA&A*, **17**, 73

Soifer, B.T., *et al.* 1986, *ApJ*, **304**, 651

van de Hulst, H.C. and De Jong, T. 1969, *Physica* **41**, 151

Walterbos, R.A.M. 1988, in *Galactic and Extragalactic Star Formation*, eds. R.E. Pudritz and M. Fich, Kluwer, Dordrecht, p361

Walterbos, R.A.M. and Kennicutt, R.C. 1987, *A&AS*, **69**, 311

Walterbos, R.A.M. and Schwering, P.B.W. 1987, *A&A*, **180**, 27

Xu, C. and Helou, H. 1993a, to appear in *Infrared Cirrus and Diffuse Interstellar Clouds*, eds. R. Cutri and W. Latter

Xu, C. and Helou, H. 1993b, in preparation